Effects of divergent ghost loops in the presence of dynamical quarks

Clara T. Figueiredo, A. C. Aguilar

Instituto de Física Gleb Wataghin, Universidade Estadual de Campinas

Introduction

Recently it was established that, in the Landau gauge, there exists a profound connection among certain characteristics of the Green's functions of QCD, whose origin is related to the masslessness of the ghost field [1]. More specifically, the ghost loop displays a IR divergence, due to the fact that the ghost field does not acquire a nonperturbative mass. It was shown in Ref. [1] that at least two Green's functions, namely the gluon propagator and the three gluon vertex, are directly affected by such divergence. However, these effects were analyzed in the context of a pure Yang-Mills theory (no quarks). In this poster, we will reproduce the results obtained in Ref. [1] and, then, we will present our initial steps towards the inclusion of the quark fields into the analysis. The aim is to observe the impact of the ghost loop divergence in the IR behavior of the gluon propagator and in the three-gluon vertex in the presence of the quark fields.

General Considerations

We start with the definition of the full gluon propagator, which in the Landau gauge is given by

$$i\Delta_{\mu\nu} = -iP_{\mu\nu}(q)\Delta(q^2)\,; \qquad P_{\mu\nu}(q) = g_{\mu\nu} - \frac{q_\mu q_\nu}{q^2}\,. \tag{1}$$

It is known that the gluon propagator is finite in the IR region [2–5]. Such behavior is due to a dynamically generated gluon mass, so that the scalar function $\Delta(q^2)$ can be decomposed as (Euclidean space)

$$\Delta^{-1}(q^2) = q^2 J(q^2) + m^2(q^2)\,, \tag{2}$$

where $J(q^2)$ is the inverse of the gluon dressing function and $m^2(q^2)$ is the dynamically generated gluon mass.

On the other hand, the ghost propagator remains massless nonperturbatively. In particular, we can define the ghost propagator as being $D(q^2) = F(q^2)/q^2$. Although the ghost dressing function, $F(q^2)$, is IR finite [2–5], we can easily see that $D(q^2)$ diverges as $q^2 \to 0$.

In the PT-BFM framework, the quenched Schwinger-Dyson equation (SDE) for the QB (quantum-background) gluon propagator, $\widetilde{\Delta}(q^2)$, is given in Fig. 1. It is important to mention that the conventional gluon propagator $\Delta(q^2)$ is related to the $\widetilde{\Delta}(q^2)$ by

$$[1 + G(q^2)]\Delta^{-1}(q^2) = \widetilde{\Delta}^{-1}(q^2), \tag{3}$$

where $1 + G(q^2)$ is an auxiliary function typical from the PT-BFM formalism. In particular, here we will employ the approximation that $1 + G(q^2) \approx F^{-1}(q^2)$.

Note that Eq. (3) is satisfied separately by the kinetic and the mass terms; thus, using the approximation above mentioned, we have

$$J(q^2) = F(q^2)\widetilde{J}(q^2); \qquad m^2(q^2) = F(q^2)\widetilde{m}^2(q^2). \tag{4}$$

It is easy to show that the diagram (a_3) has a divergent term proportional to $\ln(q^2)$ for $d = 4$, whereas the diagram (a_1) remains finite, since it is proportional to $\ln(q^2 + m^2(q^2))$.

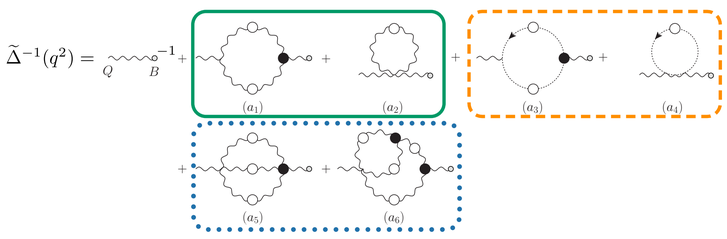

Fig 1: SDE obeyed by the QB gluon propagator in a quenched theory. Black (white) blobs represent fully dressed 1-PI (connected) Green's functions. [1]

Toy Model

In order to understand, in a simpler context, the effects of the above mentioned ghost loop divergence, one can use a *toy model* in 1-loop. Within this simple model, we insert a "hard" mass for the gluon, so that we can see the qualitative effects in the Green's functions of the theory.

In this case, the kinetic terms can be written as

$$J_{a_1}(q^2) \sim \ln\left(\frac{q^2+m^2}{\mu^2}\right)\,; \qquad J_{a_3}(q^2) \sim \ln\left(\frac{q^2}{\mu^2}\right)\,. \tag{5}$$

The corresponding gluon propagator is given by

$$\Delta^{-1}(q^2) = q^2[1 + c_1 J_{a_1}(q^2) + c_3 J_{a_3}(q^2)] + m^2\,, \tag{6}$$

where

$$c_1 = 2\left(\frac{\alpha_s C_A}{4\pi}\right)\,; \qquad c_2 = \frac{1}{6}\left(\frac{\alpha_s C_A}{4\pi}\right)\,, \tag{7}$$

with $\alpha_s = g^2/4\pi$ and C_A the Casimir eigenvalue in the adjoint representation.

The divergence of the $J_{a_3}(q^2)$ term implies that the first derivative of $\Delta(q^2)$ diverges when $q \to 0$,

$$\begin{aligned}\left[\Delta^{-1}(q^2)\right]' &= \left[q^2 J(q^2)\right]' \\ &= c_2 \ln\left(\frac{q^2}{\mu^2}\right) + \left\{1 + c_1 \ln\left[\frac{(q^2+m^2)}{\mu^2}\right] + \frac{c_1\, q^2}{q^2+m^2} + c_2\right\}\,.\end{aligned}$$

The quantity in curly brackets is finite. Besides, for $q^2 > \mu^2$, it is also positive definite, and so is the massless logarithm. However, as $q^2 \to 0$, the first term becomes arbitrarily large and negative. Consequently, there exists a value $0 < q^2_\Delta < \mu^2$ such that $[\Delta^{-1}(q^2_\Delta)]' = 0$. This corresponds to a minimum of $\Delta^{-1}(q^2)$ since $[\Delta^{-1}(q^2)]'' > 0$.

Now, to observe the effects of the ghost divergence in the three gluon vertex, we have to link the gluon kinetic term with lattice simulations of the three-gluon vertex. To do that, we introduce the R-projector [7], defined as

$$R(q,r,p) = \frac{\mathbf{N}(q,r,p)}{\mathbf{D}(q,r,p)}\,, \tag{8}$$

where

$$\begin{aligned}\mathbf{N}(q,r,p) &= \Gamma^{(0)}_{\alpha\mu\nu}(q,r,p)P^{\alpha\rho}(q)P^{\mu\sigma}(r)P^{\nu\tau}(p)\Gamma_{\rho\sigma\tau}(q,r,p)\,, \\ \mathbf{D}(q,r,p) &= \Gamma^{(0)}_{\alpha\mu\nu}(q,r,p)P^{\alpha\rho}(q)P^{\mu\sigma}(r)P^{\nu\tau}(p)\Gamma^{(0)}_{\rho\sigma\tau}(q,r,p)\,.\end{aligned} \tag{9}$$

From the kinetic point of view, R depends on the modulo of two independent momenta (q^2 and r^2) and the angle φ between them. It is usual to analyze the orthogonal configuration in which $\varphi = \pi/2$ and $r^2 = 0$. Using the WIs in the PT-BFM formalism, it is possible to establish that [1]

$$R(q^2) \sim [q^2 J(q^2)]'\,. \tag{10}$$

Therefore, in the toy model, the point q_0 where R goes from positive to negative values corresponds exactly to the location of the minimum of $\Delta^{-1}(q^2)$, q_Δ. In addition, within the toy model the minimum of the kinetic term $q^2J(q^2)$, q_j, corresponds to a maximum of the propagator $\Delta(q^2)$. These coincidences, however, only occur because we set a constant gluon mass.

Full Nonperturbative Analysis

In the full nonperturbative analysis, we consider the momentum dependent dynamical gluon mass, $m^2(q^2)$. One may separate the contributions to the kinetic term $J(q^2)$ into two types: those originating from gluon loops, such as (a_1) and (a_2) and those originating from ghost loops (a_3) and (a_4); we will denote them, respectively, as $J_g(q^2)$ and $J_c(q^2)$. Then, we have

$$J(q^2) = 1 + J_g(q^2) + J_c(q^2)\,. \tag{11}$$

Since $J_g(q^2)$ is finite as $q^2 \to 0$, $J_c(q^2)$ presents the leading contribution. More specifically we can write

$$q^2 J_c(q^2) = 4T(q^2) - q^2 S(q^2)\,, \quad C_d = \frac{g^2 C_A}{2(d-1)}\,, \tag{12}$$

where

$$\begin{aligned}T(q^2) &= C_d F(q^2)\int_k \frac{F(k+q)-F(k)}{(k+q)^2-k^2} + C_d F(q^2)\left(\frac{d}{2}-1\right)\int_k \frac{F(k)}{k^2}, \\ S(q^2) &= \underbrace{C_d F(q^2)\int_k \frac{F(k)}{k^2(k+q)^2}}_{J^l_c(q^2)} - C_d F(q^2)\int_k \frac{F(k+q)-F(k)}{k^2[(k+q)^2-k^2]}.\end{aligned}$$

Notice that $J_c(q^2)$ can be divided into the leading part in the IR, $J^l_c(q^2)$, and the remaining subleading terms, $J^{sl}_c(q^2)$,

$$J_c(q^2) = J^l_c(q^2) + J^{sl}_c(q^2)\,, \tag{13}$$

From Eqs. (11) and (13), we obtain

$$\left[q^2 J(q^2)\right]' = J^l_c(q^2) + \left\{1 + q^2 J'(q^2) + J^{sl}_c(q^2)\right\}\,. \tag{14}$$

As in the toy model, the quantity in curly brackets is a finite contribution. Additionally, the derivative of Eq. (14) is positive in the UV and negative in the IR, so there exists a point q_j in which

$$\left[q^2 J(q^2)\right]'_{q=q_j} = 0\,. \tag{15}$$

However, the location of q_j cannot be determined precisely, because we do not know all the terms inside the curly brackets of Eq. (14). Nonetheless, its value can be obtained from the combination $\Delta^{-1}(q^2) - m^2(q^2)$.

To verify the existence of the maximum of $\Delta(q^2)$, we recall that

$$\left[\Delta^{-1}(q^2)\right]' = \left[q^2 J(q^2)\right]' + \left[m^2(q^2)\right]'\,. \tag{16}$$

We know, from the equation that governs $m^2(q^2)$, obtained in [6], that the IR divergence of $J^l_c(q^2)$ is not canceled by a similar divergence in $\left[m^2(q^2)\right]'$. Therefore the gluon propagator presents a maximum at q_Δ. It is also possible to show that $q_j < q_\Delta$ [1].

In Fig.2 and Fig.3 we reveal the numerical results for the various components of the gluon propagator for the quenched full nonperturbative analysis.

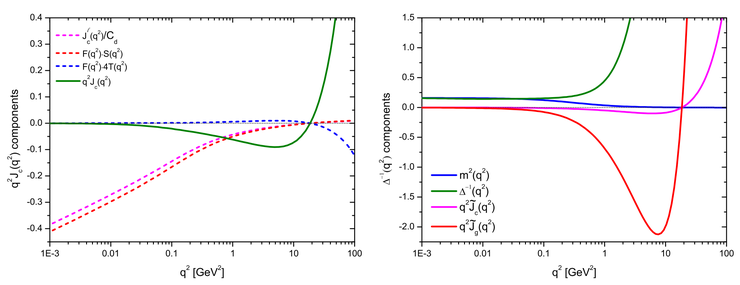

Fig 2: The ghost loop contribution, $q^2J_c(q^2)$, to the gluon kinetic term $q^2J(q^2)$ (left panel). The gauge invariant decomposition of the gluon propagator (right panel).

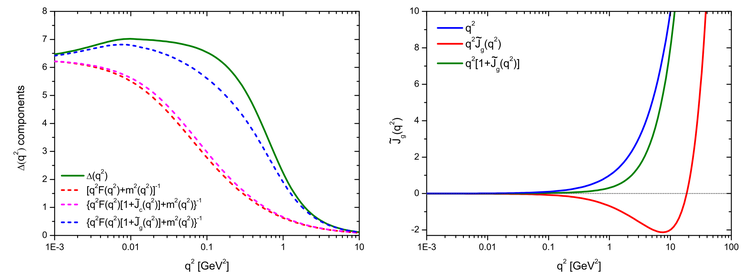

Fig 3: The partial contributions of the gluon propagator (left panel). Contributions to the invariant gluon kinetic term $q^2\tilde{J}(q^2)$ (right panel).

The Toy Model with Quarks

The techniques developed previously can be applied to the unquenched case through the modification $\Delta_Q^{-1}(q^2) - m_Q^2(q^2) = q^2(J_c + J_g + J_Q)$, where q^2J_Q is the quark loop (finite in the IR) and $\Delta_Q^{-1}(q^2)$ and $m_Q^2(q^2)$ represent, respectively, the inverse propagator and the unquenched dynamical mass. The quark loop diagram that contributes to the gluon propagator is given in Fig. 4.

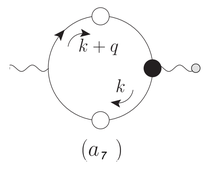

Fig 4: Diagram representing the quark loop contribution to the SDE of the gluon propagator.

Including the quark loop in the toy model, we have

$$\Delta_Q^{-1}(q^2) = q^2\left[1 + c_1 J_{a_1}(q^2) + c_2 J_{a_3}(q^2) + c_3 J_{a_7}(q^2)\right] + m^2\,. \tag{17}$$

In the UV limit for $d = 4$, we know that

$$J_{a_7} \sim \ln\left(\frac{q^2+M^2}{\mu^2}\right)\,; \qquad c_3 = -\frac{4}{3}n_f\frac{\alpha_s}{8\pi} \tag{18}$$

where M is the quark mass (not momentum dependent for now) and n_f is the number of active quarks.

The effects of the above changes in the toy model can be observed in Fig. 5 and 6, where we compare the results for the quenched and unquenched cases.

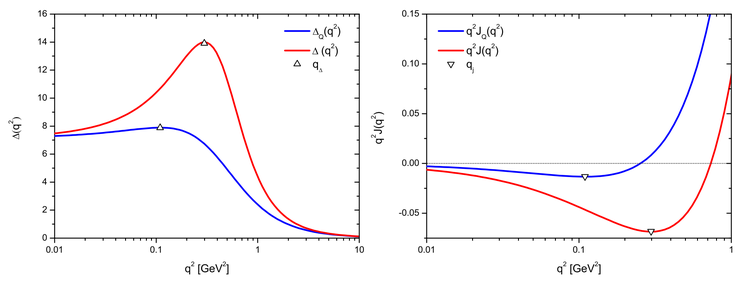

Fig 5: Gluon propagator $\Delta(q^2)$ and its kinetic part $q^2J(q^2)$. We have $m^2 = 0.14\,GeV^2$, $M^2 = 0.09\,GeV^2$, $\mu^2 = 18.64\,GeV^2$, $n_f = 2$ e $\alpha_s = 0.629$. The location of the points q_Δ and q_j is marked in the graphs.

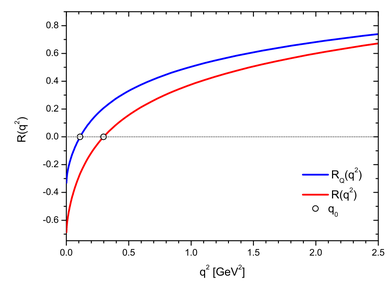

Fig 6: The corresponding $R(q^2)$ projector. The point q_0 is marked by a circle in the graph.

Conclusions

From Fig 6, we notice that when the quark loop is added to the toy model, the relevant points, q_Δ, q_j, and q_0, are shifted towards the IR region. The next step of this work is to complete the full nonperturbative calculations in order to verify whether the same pattern persists. We expect to find a quantitative difference from the full nonperturbative quenched case, but not a qualitative one, since the origin of the general effects is related exclusively to the presence of the massless ghost loops.

References

[1] A. C. Aguilar, D. Binosi, D. Ibañez and J. Papavassiliou, Phys. Rev. D **89**, no. 8, 085008 (2014).

[2] A. C. Aguilar, D. Binosi and J. Papavassiliou, Phys. Rev. D **78**, 025010 (2008).

[3] P. Boucaud, J. P. Leroy, A. Le Yaouanc, J. Micheli, O. Pene and J. Rodriguez-Quintero, JHEP **0806**, 099 (2008).

[4] A. Cucchieri and T. Mendes, PoS LAT **2007**, 297 (2007).

[5] I. L. Bogolubsky, E. M. Ilgenfritz, M. Muller-Preussker and A. Sternbeck, Phys. Lett. B **676**, 69 (2009).

[6] D. Binosi, D. Ibanez and J. Papavassiliou, Phys. Rev. D **86**, 085033 (2012).

[7] A. Cucchieri, A. Maas and T. Mendes, Phys. Rev. D **74**, 014503 (2006); Phys. Rev. D **77**, 094510 (2008).